

Bachelor Thesis

A STUDY TO THE EFFECT OF COBALT-DOPING ON HYBRID SILICA MEMBRANES

Rik Eijkelenkamp

FACULTY OF SCIENCE AND TECHNOLOGY
INORGANIC MEMBRANES

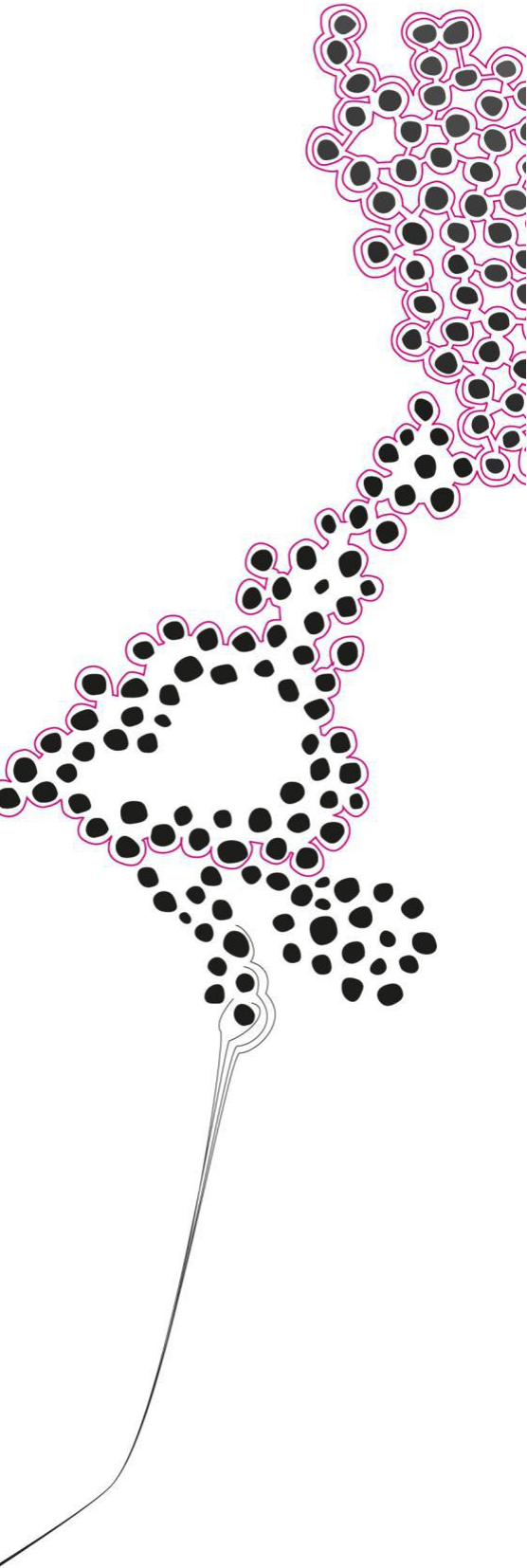
Examination Committee

Prof. Dr. Ir. A. Nijmeijer

Dr. A.J.A. Winnubst

Dr. ir. G. Koster

M. ten Hove, MSc



Abstract

The focus of this research was to study the effect of cobalt-doping on the structure and performance of hybrid silica membranes made with 1,2-bis(triethoxysilyl)ethane (BTESE) as precursor. Sols were made with cobalt concentrations between 7 and 28 mol% and varying amounts of nitric acid and measured for particle size and particle size distribution in a dynamic light scattering apparatus. Cobalt concentrations above 16% gave a bimodal particle size distribution, cobalt concentration of 16% and below gave a mono modal size distribution with particles between 7 and 14 nm. Sols with different dilutions were measured for particle size and showed a decrease in measured particle size when de sol was diluted from 0 times to 15 times. When the sols were diluted more than 15 times the distribution became bimodal.

XRD experiments were done on 16% and 22% samples calcined at 400°C in a nitrogen environment. No peaks were found, indicating an amorphous structure which suggest that the cobalt was incorporated in the silica matrix or existed in particles with a non crystalline structure.

Single gas permeation experiments were done on 16 mol% cobalt concentration membranes of sols that were diluted 6 and 10 times. The gas permeation data of these membrane were compared to a membrane without cobalt doping and turned out to be higher suggesting a more open structure than standard BTESE membranes. Permselectivity turned out to be lower for H_2/N_2 and H_2/CH_4 and higher for H_2/CO_2 for both the six and ten times diluted sols if compared with standard BTESE. From the cobalt-doped membranes only the H_2/CH_4 permselectivity was close to two times higher for the ten times diluted sol compared to the six times diluted sol indicating that the membrane made of the more diluted sol had less defects.

Table of Contents

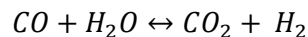
1	Introduction	4
1.1.	State of the art in membranes	5
1.1.1.	Silica membranes.....	5
1.1.2.	Hybrid silica	5
1.1.3.	Metal Doping.....	6
1.2.	Goal of the research.....	7
2	Theory.....	8
2.1.	Sol-gel chemistry.....	8
2.2.	Transport	9
2.3.	Particle size.....	10
3	Experimental.....	12
3.1.	Synthesis.....	12
3.2.	Membrane fabrication	13
3.3.	Characterization.....	13
3.3.1.	Dynamic light scattering (DLS)	13
3.3.2.	X-ray diffraction (XRD).....	14
3.3.3.	Permeation set-up	14
4	Results and discussion.....	15
5	Conclusion.....	22
6	Recommendations	23
7	References	24

1 Introduction

Every year the demand for energy increases. From 2010 to 2035 the total energy demand is estimated to increase by 47 percent.[3] This increase in energy consumption has a large impact on the environment because of the use of fossil fuels for the production of energy. An increase in energy consumption causes an increase in the burning of fossil fuels which increases the amount of CO₂ released into the air. While the CO₂ production increases, the rules on CO₂ emissions are getting stricter so the search for a cleaner energy production is becoming more important.

One of the potential solution for a cleaner energy production which is getting a lot of attention in contemporary research is the usage of hydrogen as a fuel because its combustion product is only water. Two options to produce hydrogen are coal gasification and steam methane reforming, both followed by the water gas shift reaction. Steam reforming is a process where methane is converted into hydrogen and carbon monoxide. Coal gasification is a process where heat and pressure break down coal into its chemical constituents. One of these constituents is hydrogen gas which is an interesting alternative to oil and natural gas for energy production, because coal is expected to outlast the gas and oil reserves.[4]

Coal gasification and steam methane reforming produce syngas (CO and H₂). To maximize the hydrogen production, the syngas needs further processing through the water gas shift reaction(WGS):



This reaction is commonly carried out at temperature between 250°C and 400°C because at these temperatures the reaction is fast. The disadvantage of higher temperatures is that the equilibrium of the reaction shifts more to the left because this reaction is exothermic ($\Delta H = -41,2$ kJ/mol) resulting in a lower conversion. After the water gas shift reaction the CO₂ is commonly separated from H₂ by pressure swing adsorption (PSA) [5].

An alternative for PSA is to combine the WGS reaction with product separation. This can be done with membranes that are selective for hydrogen. The membranes can enhance the conversion because the H₂ can be removed from the reactor, thus shifting the equilibrium to the right. Also an advantage of membranes over PSA is that for PSA the incoming gas flow needs to be cooled to 50°C which is capital intensive and this is not necessary for membrane separation.

The membranes used for this process need to be highly selective for H₂/CO₂ to create a hydrogen gas with a high purity but also need to have a high permeance for H₂ to recover large amounts of the gas with reasonable membrane surface areas. The permeance and selectivity of the membranes should not change over time, so a membrane used for H₂ production has to be stable under the water gas shift reaction conditions. This means that the membrane should be able to withstand temperatures between 250°C and 400°C and because water is involved in the reaction it should be hydrothermally stable. [6]

used in pervaporation experiments at 150 °C to test their hydrothermal stability. A feed mixture of water-n-butanol (5wt% water) resulted in a permeate containing 98wt% water and remained constant after 2 years of continuous testing [10, 13]. Membranes made with only BTESE as precursor showed a constant separation factor greater than 4000 after two years of testing with pervaporation at 150 °C [12].

It can be concluded that silica membranes with organic links have a higher chemical resistance against water and with that a higher hydrothermal stability than amorphous silica membranes and they have a higher mechanical resistance against cracks and defects because the flexibility of the organic groups decreases the internal stresses.[14]

1.1.3. Metal Doping

Nogami and Moriya reported that composite materials from silica with metal oxide showed better alkali resistance. They suggested that metal oxides can improve the stability of materials made of silica and metal oxides in a wet environment [15]. Because the stability of silica membranes was low under wet conditions, composite membranes were made to improve this stability. That was why metal ions such as aluminium, zirconium, niobium, cobalt, nickel were doped in silica membranes by different research groups and tested on their hydrothermal stability and permselectivity. The doped membranes showed an increase in stability compared to non-doped membranes [16-18].

Cobalt-doped membranes were made by several research groups by sol-gel synthesis using $Co(NO_3) \cdot 6H_2O$ and TEOS as precursor and dip coated on alumina supports. Analysis methods used were for instance: single gas permeation, multiple gas permeation, X-ray diffraction, infrared spectroscopy and pervaporation experiments. The membranes were tested for the water gas shift reaction and proved to be stable under wet conditions. However the water had a negative effect on the permselectivity of all gasses over hydrogen [19]. The single gas permeation test showed that the permeance of all gasses was temperature dependent and that the membranes possessed molecular sieving properties. When the single gas permeation test were done on the membranes after they were exposed to steam the permeance of the gasses decreased due to densification of the membrane [20]. The multiple gas permeation test showed a trade-off between permselectivity and permeance. When more gasses beside hydrogen gas were present in the feed stream the permeance of hydrogen gas decreased [21].

When the membranes made of TEOS with cobalt were tested with a gas stream containing 3 vol% water the permselectivity of helium over hydrogen increased. It increased further after regeneration of the membranes with dry helium gas streams. These effects were explained by structural changes of the silica matrix. Although the silica matrix changed, the overall integrity of the membrane remained intact and this indicated that the cobalt could counteract some of the effects of water on membranes when compared with silica systems without metal doping [8].

When the permselectivity of the cobalt-doped membranes were compared to the amorphous silica membranes it turned out that for cobalt-doped membranes the permselectivity of H_2/N_2 was more than ten times higher under hydrothermal conditions than for the non-doped membranes. From the XRD experiments done on the membranes it was concluded that the cobalt was incorporated in the network [22-24].

One can conclude that doping cobalt in membranes had a positive effect on the hydrothermal stability and the permselectivity but the water still effected the membranes resulting in densification.

1.2. Goal of the research

In the past much research has been done with cobalt doping in silica membranes with TEOS as precursor but never with cobalt doping with BTESE as precursor. In this research the effect of cobalt-doping on the structure and performance of membranes made with BTESE as precursor was studied.

The first part of the research was to study the effect of cobalt-doping on the structure. The structure of a membrane is a/o determined by the size of the colloids in the sol that was used for making the membrane and the degree of crystallinity of the membrane.

The goal was to determine the effect of acidity during sol synthesis and the effect of cobalt concentration on the particle size of the sol. It was expected that the particles in the sol made with cobalt are bigger than the particles in the sol made without cobalt when the ratios of reactants are kept the same. This was reported in literature for TEOS[23] and is expected because the coordination number of cobalt is higher [25] than that of Si [26].

For the crystallinity the aim was to determine if the amount of cobalt had an effect on the degree of crystallinity. It was expected that for low cobalt concentrations the structure is amorphous and for high cobalt concentrations the structure contains crystals because then the amount of cobalt is too high to be incorporated in the matrix.

The second part of the research was to study the effect of cobalt-doping on the performance of a membrane and to compare this to membranes made of BTESE without doping. The performance of a membrane is determined by its permselectivity and the permeances of gasses. Expected was that the permeances of all gasses would increase and the permselectivities would decrease because it is expected that the microporosity decreases while the mesoporosity increases as seen for membranes made of TEOS [27]. The performance of the membrane is affected by defects in the membrane and one goal of this research was to determine if and how the amount of diluent used in the development of the membrane would affect the amount of defects. It was expected that the amount of defects would decrease when more diluent is added because a more diluted sol can create a thinner layer which is less vulnerable for cracks or other defects.

2 Theory

A membrane is a discrete, thin interface that moderates the permeation of chemical species in contact with it and can separate molecules between 1 Å and 10 µm from smaller ones [2].

In this work ceramic membranes were used for gas separation. These ceramic membranes consist of a macro-porous support with a meso-porous intermediate layer and a thin micro-porous top layer. The support layer provides the mechanical strength and stiffness of the membrane, it is chemically inert and should have a low resistance to gas fluxes. The meso-porous layer has the purpose of providing a good surface for the separation layer. The pores of this intermediate layer should be small enough, so that the separation layer does not penetrate in it during applying of this layer by e.g. sol-gel methods but the pores of the intermediate layer should be big enough to have a low resistance for gas transport. The top layer is between 60 and 300 nm thick and has the purpose of separating gas molecules [2]. It should be thin to minimize its resistance against gas flows and free of defects because otherwise its separation abilities would decrease.

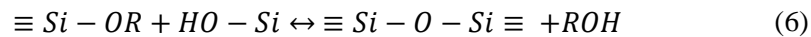
2.1. Sol-gel chemistry

Sol-gel technique is commonly used for gas-separation membrane fabrication because particle size, membrane thickness and pore size can be controlled.

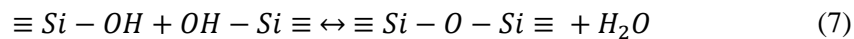
Three reactions take place when making a sol: hydrolysis, alcohol condensation and water condensation. With hydrolysis the alkyl group from the ligand from the precursor reacts with water. A hydroxyl group is formed and a small alcohol molecule is formed.



The alcohol condensation reaction binds two silica molecules through an oxygen atom. The formed bond is called a siloxane bond. The reaction occurs under the formation of an alcohol.



The water condensation reaction bonds two silica molecules through a siloxane bond under the formation of water.



As solvent commonly an alcohol is used because both water and alkoxy silanes are miscible in it. However it does influence the hydrolysis and alcohol condensation reactions because alcohol takes place in the reactions. When there is more water present the reaction shifts more to the left hand side. In this research ethanol was used.

Acids are added as catalyst in the hydrolysis step [28]. In this research nitric acid was used. The effect of acids on sols with low water:silica ratios are weakly branched sols. While base catalyzed hydrolysis

with large water:silica ratios make branched sols. Higher acid and water concentrations result in faster hydrolysis [2].

After sol creation the sols are deposited on a support by dip-coating and then dried and calcined in an oven [28].

2.2. Transport

Membranes are characterized by their ability to transport molecules. A measure for this ability is called the permeation [P_i] in [$\text{mol.m}^{-2}.\text{s}^{-1}.\text{Pa}^{-1}$] and it is calculated by dividing the molar flux of particles i [N_i] in [$\text{mol.m}^{-2}.\text{s}^{-1}$] by the pressure difference [ΔP] in [Pa].

$$P_i = \frac{N_i}{\Delta P} \quad (1)$$

The permselectivity [α] of a membrane is a measure for the membrane to separate gasses and is calculated by dividing the permeations of the gasses.

$$\alpha_{i/j} = \frac{P_i}{P_j} \quad (2)$$

Different transport mechanisms exist for membranes with pore sizes between 0,5 nm and 50 nm.

When the pore radius is smaller than the mean free path of a gas the diffusion is called Knudsen diffusion. The mean free path (λ) of common gases range from 50-200 nm so when the pore radius (r) is smaller than 50 nm the ratio between radius and mean free path (r/λ) is smaller than one and diffusion can be approximated by the Knudsen mechanism.

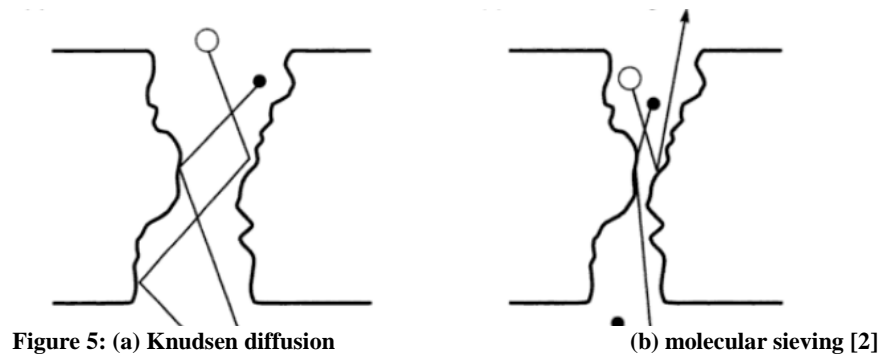
According to Knudsen the transport rate of any gas is inversely proportional to the square root of the mass of the molecules. Knudsen selectivity of a membrane implies that it is proportional to the square root of the molecular masses and is based on Graham's law which states that the square root of two are equal to the inverse ratio of their fluxes [29].

$$\alpha_{i/j} = \sqrt{\frac{M_1}{M_2}} \quad (3)$$

The permselectivity can be measured and compared to the permselectivity expected according to Knudsen. When the measured permselectivity is higher than expected by Knudsen the diffusion does not follow Knudsen diffusion and other mechanisms influence the diffusion.

Membranes with pore sizes between 0,5 nm and 1 nm can separate molecules by molecular sieving. Molecular sieving means that some molecules can pass easier through the membrane than other molecules and thus are separated from each other [9].

Figure 5 shows a schematic representation of diffusion by Knudsen and by molecular sieving where the smaller molecule passes through the membrane and the bigger molecule is bounced back.



Besides Knudsen and molecular sieving a mechanism that transports molecules through membranes is through the adsorption of gasses on its surface. This effect is non negligible for membranes with pores smaller than 10 nm. Gas molecules can adsorb on the wall of the membrane and diffuse to the other side [2].

2.3. Particle size

The hydrolysis reaction results in long branched or linear chains depending on the type of precursor used. For BTESE the chains will be branched because of the four groups attached to the silica. The entropy of the chain is highest when the chain is curled up to form a round particle because this shape has the most configurative possibilities. The particles float in the solution and it is assumed that they do not interact with each other because of repulsive forces between each other. The size of these particles is very important for making a membrane with a constant thickness and an uniform pore size. As mentioned before the particles should be bigger than the pore size of the underlying α -alumina layer and as small as possible to make a thin layer. The particle size can be measured using dynamic light scattering (DLS). DLS is a technique which measures the diffusion of particles moving under Brownian motion. Figure 6 shows a schematic representation of a DLS apparatus.

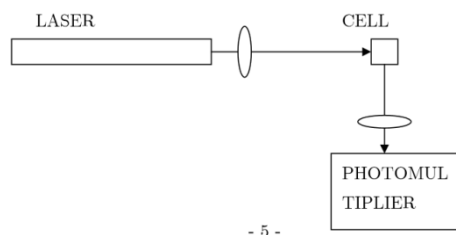


Figure 6: A schematic representation of a dynamic light scattering apparatus

A laser beam is aimed through a lens which focuses the beam in the center of the cell. The light is scattered by the particles inside the cell. The light that is scattered at a 90° angle is focused by a lens and caught by a photomultiplier. The photomultiplier converts the intensity of the incoming light into a voltaic signal. The incoming light changes with the movement of the particles because of a Doppler shift light. When the particles only move by Brownian motion the diffusion coefficient can be calculated with the displacement of the particles. The diffusion coefficient is converted into the particle size by using the Stokes-Einstein relationship:

$$D = \frac{RT}{N_A} \frac{1}{6\pi\eta r} \quad (4)$$

Where R is the gas constant N_A is Avogadro's number η is the viscosity of the fluid and r the radius of the particle. With the DLS apparatus the particle size is plotted against the intensity of the incoming light. The scattering intensity is proportional to the sixth power of the radius of the particle [26].

3 Experimental

3.1. Synthesis

All chemicals were purchased from Sigma Aldrich and no further purification methods were used. As precursor 1,2-bis(triethoxysilyl)ethane (BTESE) was used with a purity of 97%. Cobalt nitrate hexahydrate ($\text{Co}(\text{NO}_3)_2 \cdot \text{H}_2\text{O}$, $\geq 98\%$) was used as a source for the cobalt, ethanol ($\text{C}_2\text{H}_5\text{OH}$, 99,5%) was used as solvent and nitric acid (HNO_3 , 70%), was used to control the H^+ concentration of the mixture. Distilled water was used in all the experiments.

The sols were made using a reflux set-up as displayed in figure 7. A conical flask was held in water which is kept at 25°C by a heater underneath the bath coupled to a thermocouple in the water. On top of the reflux reactor a cap was placed to make sure no contaminants were able to enter the tube.



Figure 7: The set-up used for the synthesis cobalt-doped sols

For the first series of experiments the amount of cobalt nitrate hexahydrate, nitric acid and water were varied. First the cobalt nitrate hexahydrate was weighted and put in a 25 ml Conical flask. The next step was the addition of 1,77 M nitric acid. Then 5,53 ml of ethanol and various amounts of water

were added respectively. For the addition of the nitric acid, ethanol and water an Eppendorf pipette was used. The amounts used for the first experiments are displayed in table 1. The concentrations were calculated with respect to BTESE and are in mole percentage ($\text{Co}/(\text{Co}+\text{BTESE})$).

Table 1: cobalt and nitrate variation experiments

	7%	11%	16%	22%
H₂O (ml)	0,113	0,241	0,421	0,656
HNO₃ (1,77M) (ml)	2,26	1,75	1,04	0,12
Co-nitrate (g)	0,20	0,33	0,51	0,75

For the second series of experiments the amount of nitric acid was kept constant at 0,118 ml and the amount of cobalt nitrate hexahydrate was varied. The amount of added water was varied to compensate for the amount of water in the cobalt nitrate hexahydrate so the total amount of water was kept constant throughout the experiments. The mixture was supplemented to 10 ml by adding ethanol. The amounts used are displayed in table 2.

Table 2: cobalt variation experiments

	7%	12%	17%	23%	28%
H₂O (ml)	0,861	0,813	0,745	0,657	0,564
Ethanol (ml)	5,69	5,74	5,81	5,90	6,00
Co-nitrate (g)	0,20	0,33	0,51	0,75	1,00

The conical flask was put in an ice bath in order to prevent premature hydrolysis. Then 3,33 ml of BTESE was dripped carefully in the mixture and after a few minutes the mixture was set in the reflux set-up and reacted for 90 minutes. Afterwards it was taken of the set up and put back in the ice bath to stop the reaction.

3.2. Membrane fabrication

The sol was taken inside a ISO6 cleanroom. To create a thin film of the sol on the support dip coating was used. In these experiments one layer was coated on a disc shaped support of $\gamma\text{-Al}_2\text{O}_3$ on an $\alpha\text{-Al}_2\text{O}_3$ support. Before coating the sol was filtered with a 200 nm filter to collect the large particles and dripped on a Petri dish, after which air bubbles were taken out using a pipette. The support was then cleaned with an air gun and placed in the coating apparatus. In this apparatus the support spins one round and goes through the sol and ends vertically with the coated side on top where it was held for 30 seconds for the sol to dry.

The membranes were taken out of the cleanroom covered by a Petri dish to protect it from dust and taken to an oven. Subsequently they were placed in the oven and calcined at 400 °C for 3 hours under nitrogen atmosphere with ramp rates of 0,5°C per minute to consolidate the membrane.

3.3. Characterization

3.3.1. Dynamic light scattering (DLS)

In order to determine the particle size distributions of the sol DLS measurements were done with a Zetasizer nano ZS. Before they were put in the machine the sols were filtered with a filter with pores of 200 nm to take out all particles larger than 200 nm and then heated to 25 °C. Three measurements

were done with sols from 11% and 16% cobalt concentration and averaged afterwards. For the 11% sols dynamic light scattering tests were performed before and after six times dilutions. For the 16% three sols were subsequently 0, 6, 10, 15, 20 and 25 times diluted and measured in the dynamic light scattering apparatus.

3.3.2. X-ray diffraction (XRD)

Two sols of 16% and 22% cobalt concentration were dried and calcined at 400 °C under nitrogen conditions and the crystallinity was measured using XRD. These experiments were performed with a Bruker Phaser D2.

The sols were poured on a Petri dish and left in the fumehood without a lid for the ethanol to evaporate. The dried sols were put in the oven and calcined for 3 hours at 400 °C under nitrogen conditions with ramp rates of 0,5°C per minute.

The calcined flakes were ground into a powder using a mortar and placed on a holder. A XRD analysis was done starting from 10° to 90°. For the 22% sample an extra detailed measurement was conducted with a lower time increment than for the 16% sample.

3.3.3. Permeation set-up

Two sols were made for single gas permeation experiments both with 16% cobalt concentration. For the first one 8 ml sol was diluted with 50 ml ethanol and for the second one 10 ml sol was diluted with 90 ml ethanol. Per sol two membranes were coated and calcined. For reference a standard BTESE sol with the same ratios but without cobalt was synthesized, coated and calcined under the same conditions as the cobalt doped systems.

The membranes were put in the permeation set-up for single gas measurements. In the set up the membranes were clamped between two holders surrounded by a heating element and a gas was pushed through the membrane at a pressure difference of 2 bar. The gas flow was measured on the permeate side by a mass flow meter. The membrane was heated to 210 °C and cooled down to 200 °C while helium flowed through the set-up to make sure no water remained in the set-up. Then the measurements were started and stopped when the flow remained constant for five minutes for the gasses in the order: helium, nitrogen, methane, hydrogen, carbon dioxide and sulfur hexafluoride.

4 Results and discussion

In this chapter the results are presented of the experimental part. First the results of the experiments where the acidity, cobalt concentration and the amount of diluent was varied are shown. These results are displayed in the intensity distribution of the sol particles and the corresponding peak intensities. The peak intensity is the mode of the particle size distribution. Then the results from the XRD and the single gas permeation experiments are shown.

Table 3 gives the particle size peak intensities and in figure 8 the particle size distribution is plotted against the measured intensity for the experiments where the acidity is varied.

Table 3: Peak intensities of cobalt and H⁺ variation

	7%	11%	16%	22%
Co-nitrate (g)	0,2	0,33	0,51	0,75
H⁺ (mol/L)	0,355	0,285	0,178	0,0220
Intensity peak	11,8	13,8	11,7	8,6

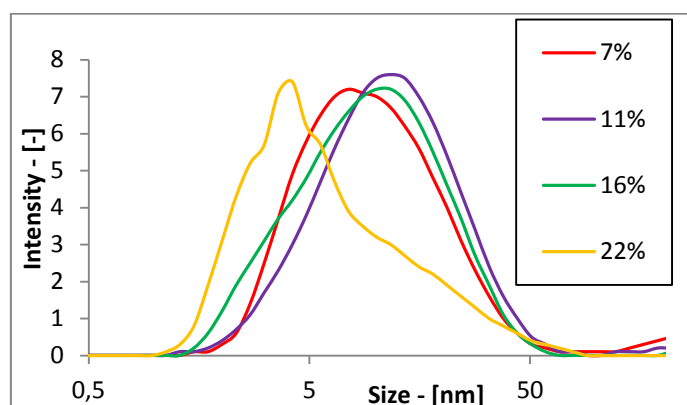


Figure 8: Intensity distribution of the sol particles of the cobalt and H⁺ variation experiments. Percentages shown are the cobalt concentrations and the corresponding H⁺ concentrations are shown in table 3

The graphs showed no clear trend for the 7%, 11% and 16% cobalt concentration. The peaks of these concentrations were broad so they have a large variation in particle size. The 11% Co-doped sol showed the peak at the largest particle size meaning that most particles were bigger than for other concentrations. The 22% Co-doped sol had a less broad particle size distribution and had a peak at a smaller particle size. The reactivity of the sol was expected to be linear with the acidity of the sample but these samples showed no such trend with the exception of the 22% Co-doped sol. This sample showed particles that were significantly smaller than the particles of the 7%, 11% and 16% Co-doped samples. The reason that no trend could be found could be because the cobalt concentration increased as the acidity decreased where the reactivity of the additional cobalt can counteract the decrease in acidity. The reactivity is expected to be higher for higher cobalt concentrations because the coordination number of cobalt is higher compared to silica particles, so more hydroxyl groups can surround the cobalt ion which can react with hydroxyl groups attached to other cobalt ions.

To study the effect of the cobalt concentration on the particle size the H^+ concentration was held constant at 0,185 mol/L in further experiments. The peak intensities from these experiments are shown in table 4 and the intensity distribution of the average of the three sols is shown in figure 9.

Table 4: Peak intensities of cobalt variation

	7%	11%	16%	22%	28%
Int Peak (nm)	8,6	7,8	8,1	9,4	15,0

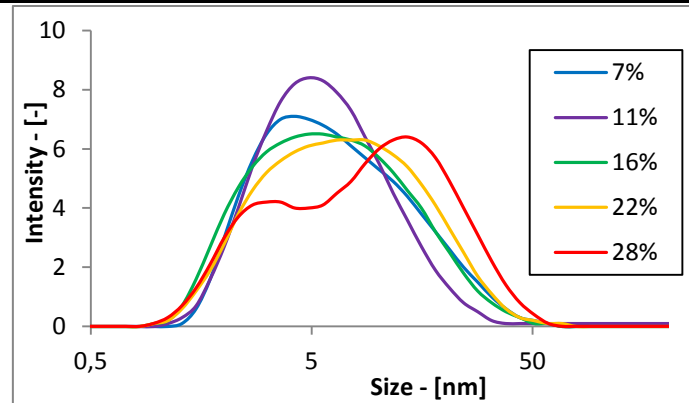


Figure 9: Intensity distribution of the sol particles of the cobalt variation experiments

The particle distributions for the various sols showed peaks becoming broader for higher cobalt concentrations and for the 22% and 28% Co-doped sols a bimodal distribution. As mentioned before, cobalt can be more reactive resulting in a more polydisperse size distribution because of its higher reactivity [26]. The broader peaks found in these experiments indicate a more polydisperse sample for higher concentrations thus confirming the expectation. An explanation for the bimodal distributions could be that when the amount of cobalt is too high to be incorporated into the silica matrix crystalline particles were formed like Co_3O_4 as reported by Esposito et. al. [27]. In our case this was however unlikely because XRD, presented below, showed no crystallinity. Another explanation of the bimodal distribution could have been by a measuring fault because commonly sols were being diluted before DLS measurements but here these sols were measured without being diluted. The Si-concentration in these experiments was 1,7 mol/L while for DLS measurements with BTESE was reported in literature concentrations between 0,25 mol/L and 0,4 mol/L were used [12]. This could give deviations in the results because the radius of the particles in the sol was calculated with the viscosity and this can change when the sol was diluted. A more diluted sol is expected to have a lower viscosity and because the diffusion coefficient remained constant the Stokes-Einstein relation (equation 4) tells us that the particle radius increases [30]. For more reliable results the DLS measurements should be done again after being diluted.

To determine whether the dilution has an influence on the measured particle size and cause deviations in the results presented above the following experiments were done. One sol contained 11% cobalt and one sol contained 16% cobalt. These DLS results of these experiments are shown below in table 5 and 6.

Table 5: Peak intensities dilution experiments for the 11% sol

	Non diluted	6x diluted
INT peak (nm)	13,8	8,7

Table 6: Intensity peaks for the dilution experiments of a 16% Co-doped sol

	6x	10x	15x	25x
Peak INT (nm)	5,8	5,4	4,1	5,5

The results showed a higher peak for the non-diluted sol for the 11% Co-doped sol and a decreasing trend for the 6x to 15x dilution of the 16% Co-doped sol. It was unlikely that the particle size changes during dilution because no reaction takes place during dilution, only extra ethanol was added. An explanation for the influence could have been the accuracy of the measuring device as mentioned before. The accuracy of the measurement can deviate because of the change in viscosity but the results were not as expected because diluting the sol resulted in a smaller measured particle size while the Stokes-Einstein relation predicts an increase in measured particle size. What could have been the reason for this result was that the motion of the particles was restricted for lower dilutions making the particles appear larger. The 0 times and 20 times diluted sols showed a bimodal distribution and because this makes the peak intensities unreliable they are not displayed in table 6. For the 25x diluted sol, the measured particle size increased. These results may be explained by deviations in the measurements because when the amount of diluent increases the amount of particles able to scatter the light per volume decrease making the measurements less accurate. More measurements should be done to be able to conclude if the results are reproducible.

The results of these experiments showed that the particles from the sol in the cobalt and nitric acid variation experiments could indeed have been deviating from the particle size expected from the data. The corresponding size distribution of these experiments is given in figure 10 and 11.

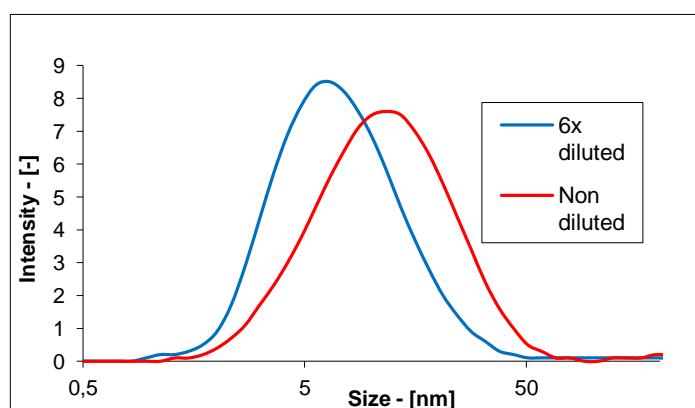


Figure 10: Intensity distribution of the 11% cobalt concentration dilution experiments

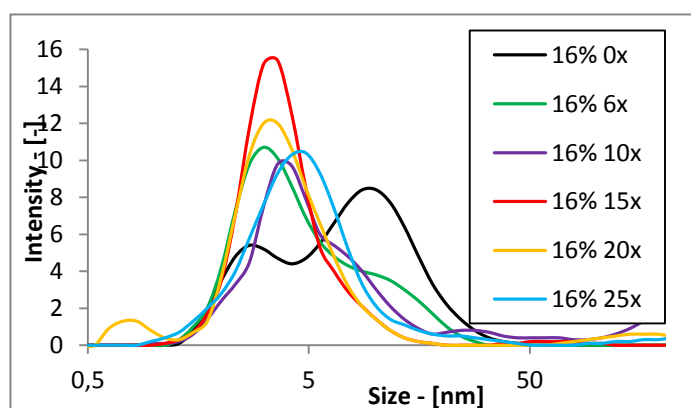


Figure 11: Intensity distribution of the 16% cobalt concentration dilution experiments

As seen in the peak intensities the less diluted sol shows peaks at larger particle sizes. For the 16% cobalt concentration sol the 6 times dilution had one irregular peak, the 10 times diluted sol had a peak that is more neat and some distortion above 200 nm which can be caused by dirt or dust. The 15 times diluted sol showed a line with a peak around 4 nm. The 20 times diluted sol had a smaller peak around 1 nm and a larger peak around 4 nm while the 25 times diluted sol showed a single peak. The graph from the 15 times dilution showed the most symmetric and narrow distribution which is best for coating a membrane. The graphs also show that more measurements should be done to be able to conclude if the results are reproducible.

A sample from the 6 and 10 times diluted sols used for coating was taken and measured in the DLS apparatus and the resulting distribution is shown in figure 12.

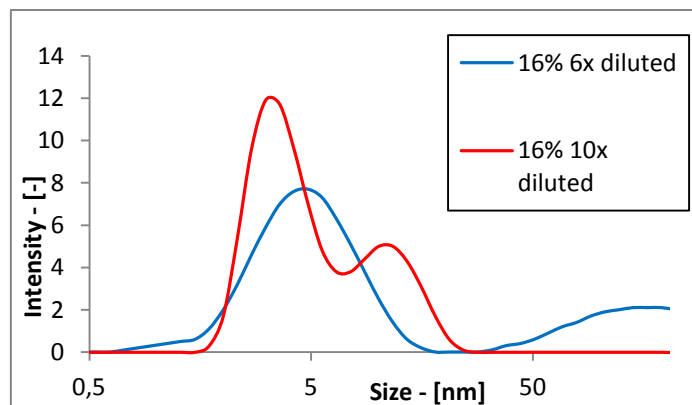


Figure 12: Intensity distribution coated sols

The distribution of the six times diluted sol showed a broad peak between 30 nm and 1000 nm. The particles above 200 nm were filtered out of the sol prior to the measurements so this peak can come from dust or dirt inside or on the outside of the cuvette and because large particles scatter significantly more than smaller particles nothing can be said about the size of the colloids in the sol. The graph showed two peaks for the 10 times diluted sol meaning that particles exist in the sol with two different sizes which is not beneficial for coating. When the particles have equal sizes the membrane made from the sols can have a uniform pore size and there is no risk of smaller particles penetration into the pores of the support. Sols with single particle size between 7 and 11 nm and a narrow particle size distribution are best for coating a membrane because they give a membrane with a uniform layer thickness and uniform pore size. These 6 and 10 times diluted sols with 16% cobalt concentration sols did not show these characteristics but due to time constraints were used for membrane coating.

Results from the XRD measurements on the 16% and the 22% Co-doped samples are shown in figure 13. The graphs were normalized and the graph of the 16% sample has a vertical offset. For the 22% Co-doped sample the time increments per angle is lowered compared to the 16% Co-doped sample resulting in a measurement with less noise.

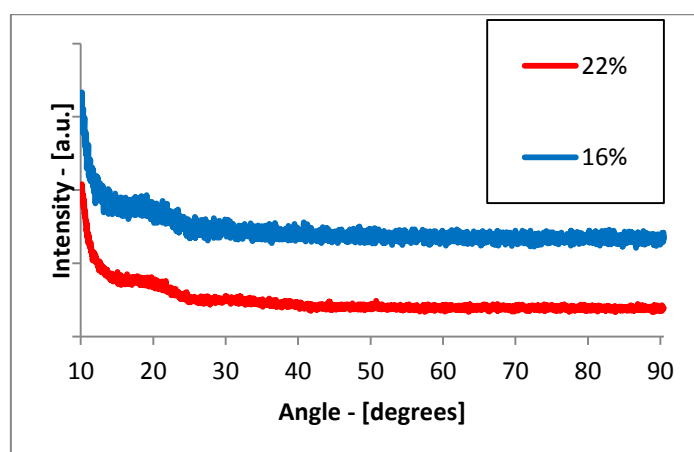


Figure 13: Results from the XRD apparatus showing no peaks for both the 22% and the 16% Co-doped samples

These samples showed no peaks over the range of 10° to 90° indicating an amorphous structure for both the 16% and the 22% Co-doped specimen. This showed that the amount of cobalt has no effect on the crystallinity for the samples in this range. Crystals could have been formed by a mechanism as proposed by Zarzosa [31]. When $Co(NO_3) \cdot 6H_2O$ is dissolved in water it can form complexes of the type $[Co(H_2O)_{6-x-y}(OH)_xO_y]$. These complexes can react with each other by hydrolysis and form

complexes where the cobalt atoms are connected to each other by an oxygen atom. When the solution is a mixture of silica and cobalt the cobalt complexes can react with silica complexes and form Si-O-Co bridges. For TEOS $\text{Si}(\text{OR})_{4-n}(\text{OH})_n$ can react with the cobalt complexes. For BTESE the mechanism can be the same because $\text{Si}_2(\text{OR})_{6-n}(\text{OH})_n$ can react with the cobalt complexes. The graph shows no presence of crystals in the samples what could be because of the low water content in the sol making the hydrolyses of cobalt complexes less likely.

Other studies [8, 23, 31] showed clear peaks for Co_3O_4 and Co_2SiO_4 between 30° and 40° and at 60° and 65° . The difference in our results and the results in other studies was probably caused by the difference in calcination process. The sols in the other researches were calcined under air or oxygen atmosphere while our samples were calcined under nitrogen atmosphere. Under these conditions the reaction between oxygen in air with cobalt cannot take place because no oxygen is available in the nitrogen atmosphere. And the calcination process in the other studies [8, 22-24, 27, 31] were conducted at temperatures between 400°C and 900°C which can result in the crystallization of the cobalt oxide. Also these studies were conducted with TEOS instead of BTESE as precursor but the peaks are expected to be at the same places when the calcination temperatures are equal because the peaks from crystalline cobalt oxide should always show up at the same angle. These XRD results indicate an amorphous structure suggesting that cobalt is incorporated in the silica matrix or as tiny crystals as reported for TEOS [22].

Sols with cobalt concentration of 16% and silica concentration before diluting of 1,7 mol/L were used for coating. Note that the cobalt concentration was calculated with respect to silica while the silica concentration was calculated with respect to the total volume of the mixture. After coating and calcining the membranes made from the six times diluted sol (6x) with a 16% cobalt concentration showed brown curved stripes on them and one of them had a possible pinhole. The membranes made from the ten times diluted sol (10x) with a 16% cobalt concentration showed no brown stripes and no pinholes were found by the naked eye.

The single gas permeation experiments showed a permeance of sulfur hexafluoride gas that was above the detection limit ($5 \cdot 10^{-10} \text{ mol/m}^2 \cdot \text{s}^{-1} \cdot \text{Pa}^{-1}$) for the 6x diluted sol membrane and below this limit for the 10x diluted sol membrane as shown in table 7. These results suggests that there were defects like pinholes present in the 6x diluted sol membrane because the kinetic diameter of the sulfur hexafluoride molecules was significantly bigger than the pore size expected for BTESE doped with cobalt based on the pore size reported for TEOS doped with cobalt [8].

Table 7: The sulfur hexafluoride permeances for the membranes made from the 6x and 10x diluted sols.

Permeance (mol/m².s.Pa)	
6x	1,9E-09
10x	Below detection limit

The gas permeation data were an average for two membranes made from the same sol plotted against the kinetic diameter of the gas molecules. These results including the permeances of the standard BTESE membrane are shown in figure 14.

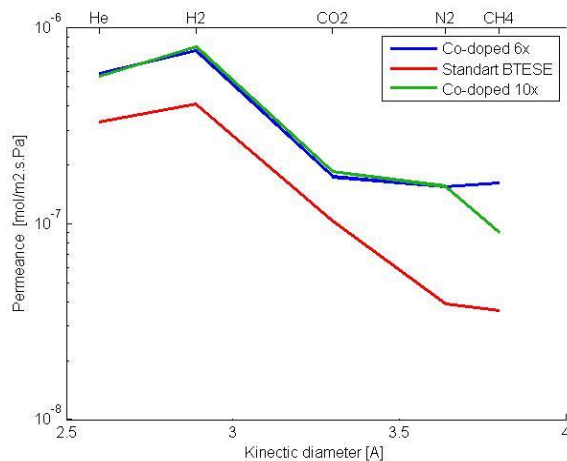


Figure 14: Single gas permeation results from membranes made of 6x and 10x diluted sol and a membrane made from a non-doped sol.

The permeances of all gasses were higher for the cobalt doped membrane than for the standard BTESE membrane. This indicates that a Co-doped membrane had a more open structure than the non-doped membrane as expected. For membranes made with TEOS doped with cobalt it is reported [27] that the mesoporosity increases and the microporosity decreases compared to non-doped membranes. The increase in mesoporosity results in an increase in permeance for all gasses. This could be an explanation for the higher permeances of Co-doped BTESE membranes compared to non-doped BTESE membranes.

For the six times diluted sol the permeation of carbon dioxide, nitrogen and methane were close to each other. An explanation for this could have been defects in the membrane or it could have been an indication that more than one mechanism was of influence on the permeance. The brown stripes and possible pinhole on the six times diluted one as mentioned before could have been the cause of the defects.

When comparing the 6x diluted with the 10x diluted cobalt-doped membranes it shows that the permeances of helium, carbon dioxide and nitrogen were close to each other. Only the permeance of methane gas was lower for the 10x diluted sol membrane than for the 6x diluted sol membrane. These results can suggest that the membrane made from the more diluted sol contained less defects like cracks or pinholes as was expected because of the thinner membrane created by the more diluted sol.

In table 8 the permselectivities of the 6 and 10 times diluted sols and of standard BTESE were displayed.

Table 8: The permselectivities of the 6x, 10x diluted sol compared to a non-doped membrane and Knudsen diffusion

	Co-doped BTESE 6x	Co-doped BTESE 10x	Standard BTESE 6x	Knudsen Diffusion
H₂/CO₂	4,4	4,4	4	4,7
H₂/N₂	5,0	5,2	10,5	3,7
H₂/CH₄	4,8	8,9	11,4	2,8

The permselectivities of the 6x diluted and the 10x diluted Co-doped membranes were lower for H_2/N_2 and H_2/CH_4 than the non-doped BTESE membranes. This means that although the permeances of all gasses was increased after doping the permeance of nitrogen and methane increased more than the permeance of hydrogen. The permselectivity of H_2/CO_2 was a bit higher for both Co-doped membranes than the non-doped membranes meaning that the permeance of CO_2 has increased less than the permeance of hydrogen.

The decrease of the H_2/N_2 and H_2/CH_4 permselectivity of the Co-doped membranes can be explained by the increase in mesoporosity because a more open structure results in a less selective membrane as mentioned before. But the increase in H_2/CO_2 permselectivity of the Co-doped membranes is unexpected. The H_2/CO_2 permselectivity is closer to the permselectivity as expected by Knudsen so it is more determined by the molecular weight difference between H_2 and CO_2 than by the size difference while the permselectivity of H_2/N_2 and H_2/CH_4 were more determined by the size difference than by the weight difference. An explanation for this behavior can be that another kind of transport has influence on the permeance of CO_2 like surface diffusion. Also the CH_4 gas stream measured on the permeate side of the membrane took a long time to become constant and could have been falsely assumed to be constant. More single gas permeation tests on Co-doped membranes should be performed to study the reproducibility of these results.

The H_2/CH_4 permselectivity was higher for the 10x diluted sol than for the 6x diluted sol which was a result of the higher CH_4 permeance for the 10x diluted sol than the 6x diluted sol. So this can come from the 10x diluted sol containing less defects.

For both six times and ten times diluted sols the H_2/CO_2 was lower than Knudsen diffusion and H_2/N_2 and H_2/CH_4 was higher than Knudsen. The membranes did not show Knudsen diffusion, but did show molecular sieving properties for H_2/CH_4 .

5 Conclusion

In this research four membranes were made with 16% cobalt concentration from 6 and 10 times diluted sols. The two sols were successfully coated on a γ -AlO₃ supported α -AlO₃ membrane. The sols were tested on the effect of acidity, cobalt concentration and amount of diluent on the particle size and the degree of crystallinity was studied by XRD. The membrane performance was studied with single gas permeation.

No trend has been found for the effect of acidity of the sol on the particle size because the effect could have been counteracted by the effect of the cobalt concentration on the particle size. The effect that cobalt concentration had on the particle size was that an increase in cobalt concentration caused the particle distribution to broaden meaning that more particles of different sizes were created.

From experiments with different amounts of diluent could have been concluded that the measured particles size is effected by the amount of diluent. No clear trend had been found but it was apparent that the measured particle size is lower for the more diluted sols in the dilution range of 0 to 15 times.

The cobalt concentration had no effect on the crystallinity of samples with cobalt concentrations of 16% and 22%. The samples were amorphous suggesting that the cobalt was incorporated in the silica matrix or exist in some non crystalline form in the membrane.

Permeation experiments with these samples showed a higher permeation for all gasses compared to standard BTESE. This indicated that the cobalt effected the structure of the membranes making it less dense than membranes made without cobalt doping.

Concluded was that the effect of cobalt on the permselectivity resulted in lower H₂/N₂ and H₂/CH₄ and higher H₂/CO₂ permselectivities when compared to a standard BTESE membrane. Meaning that standard BTESE membrane were better at separating nitrogen and methane from hydrogen while the cobalt-doped membranes were a bit better at separating hydrogen from CO₂. The cobalt-doped membranes showed no Knudsen diffusion but did show molecular sieving properties for H₂ over CH₄.

When the sol was more diluted before coating, the methane and sulfur hexafluoride permeances decreased so one can conclude that the more diluted sol had less defects/larger pores than the less diluted sol.

In general the structure of a cobalt-doped membrane was more open compared to a non-doped membrane and this had effect on the performance in a way that the permeance increased for all gasses and the selectivity only increased slightly for H₂/CO₂ but decreased for H₂/N₂ and H₂/CH₄.

6 Recommendations

To see the effect of acidity on the particle size the amount of nitric acid in the mixture should be varied while keeping the water, BTESE and cobalt ratios the same. Expected was that the particle size will increase with increasing acidity as reported for non-doped BTESE [28].

To get an accurate measure of the particle size in the sol experiments should be performed to determine the viscosity of the sol at different dilutions. In these experiments the viscosity was not measured and an approximate was used which can give, because of the use of the Stokes-Einstein equation, a deviation in the measured particle size.

To know where in the mixture the cobalt is Fourier Transform infrared experiments should be performed on a sample. It gives information about what bonds are present in the membrane so whether cobalt has formed bonds with silica or oxide or whether it has formed bonds with other cobalt atoms. The bond information can be an indication whether the cobalt is incorporated in the silica matrix or not.

The aim is to make a membrane that is hydrothermally stable and this can only be checked in a wet environment. Gas permeation experiments should be performed with water vapor and the permeability should be measured during and afterwards to see if the water vapor has an effect on the membrane.

Single gas permeation experiments with varying temperature should be performed to find the apparent activation energy. When the activation energy is known one can conclude if the transport through the membrane is activated transport and with that if the permselectivity of the gasses can be influenced by temperature. Also binary gas permeation experiments should be performed to find the true selectivity of the membrane because in some cases the selectivity is not the same as the permselectivity i.e. the permeances of the single gasses divided by each other and the goal is to separate a gas mixture. When a mixture of two gasses is used one gas can influence the surface interaction of the other gas resulting in different permeances if compared with pure gases [2]. This is of influence when transport is largely determined by surface diffusion which was expected not to be the case for these membranes.

In this work single gas permeation experiments were performed with membranes with 16 mol% of cobalt and two different dilutions because they showed an uniform intensity distribution and a particle size between 8 and 12 nm. The 7% and 11% Co-doped sols were close to these conditions and could be used for the coating of membranes but due to time constraints no experiments with these membranes. To see what the effect of the cobalt concentration on the permeance is one should develop membranes with different cobalt concentrations and perform single gas permeation experiments on them.

7 References

1. <http://withfriendship.com/images/d/17818/Silica-gel-image.jpg>.
2. Baker, R.W. and W.B. Richard, *Membrane technology and applications* 2004, Chichester [etc.]: Chichester etc. : Wiley.
3. Administration, U.S.E.I., *Annual energy outlook 2012 with projections to 2035*. 2012.
4. Shahriar Shafiee, E.T., *When will fossil fuel reserves be diminished?* Energy Policy 37, 2009. **181–189**.
5. Ribeiro, A.M., et al., *Pressure Swing Adsorption Process in Coal to Fischer–Tropsch Fuels with CO₂ Capture*. Energy & Fuels, 2012. **26(2)**: p. 1246-1253.
6. Diniz da Costa, J.C., G.P. Reed, and K. Thambimuthu, “*High Temperature Gas Separation Membranes in Coal Gasification*”. Energy Procedia, 2009. **1(1)**: p. 295-302.
7. Uhlhorn, R.J.R., *High permselectivities of microporous silica-modified γ -alumina membranes*. Journal of materials science, 1989. **letters 8**: p. 1135 I138.
8. Uhlmann, D., et al., *Cobalt-doped silica membranes for gas separation*. Journal of Membrane Science, 2009. **326(2)**: p. 316-321.
9. Vos, R.M.d. and H. Verweij, *High-Selectivity, High-Flux Silica Membranes for Gas Separation*. Science, 1998. **279(5357)**: p. 1710-1711.
10. Castricum, H.L., et al., *Hydrothermally stable molecular separation membranes from organically linked silica*. Journal of Materials Chemistry, 2008. **18(18)**: p. 2150.
11. Tsapatsis, M., *Tsapatsis structure and aging characteristics*. Journal of Membrane Science, 1994. **87**: p. 281-296.
12. Castricum, H.L., et al., *High-performance hybrid pervaporation membranes with superior hydrothermal and acid stability*. Journal of Membrane Science, 2008. **324(1-2)**: p. 111-118.
13. Castricum, H.L., et al., *Hybrid ceramic nanosieves: stabilizing nanopores with organic links*. Chem Commun (Camb), 2008(9): p. 1103-5.
14. Dubois, G., et al., *Molecular Network Reinforcement of Sol–Gel Glasses*. Advanced Materials, 2007. **19(22)**: p. 3989-3994.
15. Nogami, Y.M.a.M., *HYDRATION OF SILICATE GLASS IN STEAM ATMOSPHERE*. Journal of Non-Crystalline Solids, 1980. **38 & 39**: p. 667-672.

16. Tsuru, T., *Silica-zirconia membranes for nanofiltration*. Journal of Membrane Science, 1997. **149**: p. 127-135.
17. Fotou, G.P., Y.S. Lin, and S.E. Pratsinis, *Hydrothermal stability of pure and modified microporous silica membranes*. Journal of Materials Science, 1995. **30**(11): p. 2803-2808.
18. Qi, H., et al., *Effect of Nb content on hydrothermal stability of a novel ethylene-bridged silsesquioxane molecular sieving membrane for H₂/CO₂ separation*. Journal of Membrane Science, 2012. **421-422**: p. 190-200.
19. Battersby, S., et al., *Metal doped silica membrane reactor: Operational effects of reaction and permeation for the water gas shift reaction*. Journal of Membrane Science, 2008. **316**(1-2): p. 46-52.
20. Battersby, S., et al., *Hydrothermal stability of cobalt silica membranes in a water gas shift membrane reactor*. Separation and Purification Technology, 2009. **66**(2): p. 299-305.
21. Battersby, S., et al., *Performance of cobalt silica membranes in gas mixture separation*. Journal of Membrane Science, 2009. **329**(1-2): p. 91-98.
22. Tsuru, T., *Development of Metal-doped Silica Membranes*. J. Jpn. Petrol. Inst., 2011. **Vol. 54**(No. 5): p. 277-286.
23. Wang, J. and T. Tsuru, *Cobalt-doped silica membranes for pervaporation dehydration of ethanol/water solutions*. Journal of Membrane Science, 2011. **369**(1-2): p. 13-19.
24. Igi, R., et al., *Characterization of Co-Doped Silica for Improved Hydrothermal Stability and Application to Hydrogen Separation Membranes at High Temperatures*. Journal of the American Ceramic Society, 2008. **91**(9): p. 2975-2981.
25. <http://bilbo.chm.uri.edu/PeriodicTable/cobalt.htm>.
26. Boffa, V., et al., *Microporous niobia-silica membranes: Influence of sol composition and structure on gas transport properties*. Microporous and Mesoporous Materials, 2009. **118**(1-3): p. 202-209.
27. Esposito, S., et al., *Cobalt-silicon mixed oxide nanocomposites by modified sol-gel method*. Journal of Solid State Chemistry, 2007. **180**(12): p. 3341-3350.
28. Brinker, C.J. and C. Brinker, *Sol-gel science : the physics and chemistry of sol-gel processing*, ed. G.W.j.a. Scherer 1990, Boston [etc.]: Boston etc. : Harcourt Brace Jovanovich.
29. Mason, E.A., *Graham's Laws of Diffusion and Effusion*. Journal of Chemical Education, 1967. **44**(Number 12).
30. Goldberg, W.I., *Dynamic light scattering*. Am. J. Phys., 1999. **67**: p. 12.

31. Ortega Zarzosa, G., *Cobalt Oxide/Silica Xerogels Powders: X-Ray Diffraction, Infrared and Visible Absorption Studies*. Journal of sol-gel science and technology, 2002. **24**(1): p. 23-29.